A study on locating the sonic source of sinusoidal magneto-acoustic signals using a vector method

Shunqi Zhang, Xiaoqing Zhou, Ren Ma, Tao Yin and Zhipeng Liu[*]
Institute of Biomedical Engineering, Chinese Academy of Medical Sciences & Peking Union Medical College, Tianjin 300192, China

Abstract. Methods based on the magnetic-acoustic effect are of great significance in studying the electrical imaging properties of biological tissues and currents. The continuous wave method, which is commonly used, can only detect the current amplitude without the sound source position. Although the pulse mode adopted in magneto-acoustic imaging can locate the sonic source, the low measuring accuracy and low SNR has limited its application. In this study, a vector method was used to solve and analyze the magnetic-acoustic signal based on the continuous sine wave mode. This study includes theory modeling of the vector method, simulations to the line model, and experiments with wire samples to analyze magneto-acoustic (MA) signal characteristics. The results showed that the amplitude and phase of the MA signal contained the location information of the sonic source. The amplitude and phase obeyed the vector theory in the complex plane. This study sets a foundation for a new technique to locate sonic sources for biomedical imaging of tissue conductivity. It also aids in studying biological current detecting and reconstruction based on the magneto-acoustic effect.

Keywords: Magneto-acoustic effect, vector method, sonic source locating, amplitude, phase

1. Introduction

This study proposes a new method based on the magneto-acoustic effect for imaging electrical parameters of biological tissue [1] and sensing biological micro-currents [2].

In this magneto-acoustic method, tissue was placed in a magnetic field, and an electrode or coil produced a time-varied current. Then, the vibrations produced by Lorentz force [3-5] emitted magneto-acoustic (MA) signals, which could be detected and measured outside the sample. Thus, measuring the MA signal can reveal the conductivity [6] or the tissue's current [7].

In this method, electrical parameters of biological tissue samples were converted into a sonic signal. Measuring sonic waves is easier than measuring electromagnetic waves because sonic waves transmit at a much slower rate. Also, this method can avoid the dispersion effect caused by an electrical current. As a result, the magneto-acoustic method makes it possible to locate the sonic source with high

---

    *Address for correspondence: Zhipeng Liu, Institute of Biomedical Engineering, Chinese Academy of Medical Sciences & Peking Union Medical College, No. 236 Baidi Road, Nankai District, Tianjin 300192, China. Tel.: +8622-87891982; Fax: +8622-87892951; E-mail: lzpeng67@163.com.

precision.

The current magneto-acoustic imaging method uses high voltage short pulse excitations and the receiving method to achieve high accuracy of sound source localization [8, 9]. This mode makes the sonic source easy to distinguish from MA signals. However, the excitation is difficult to manufacture and poses safety risks. Also, it is susceptible to high-frequency pulse interference during the detection process [10]. These factors limit pulse mode detection accuracy, and the signal-to-noise ratio (SNR) is low.

Using the continuous wave mode in biological current detection [11] and electrical parameter measurements [12] achieves high detection accuracy [13], but it has not yet been used to locate the sonic source of currents or accurately reconstruct the neural current of biological tissue [7].

In this paper, the vector method is proposed to compute and analyze the MA signal using continuous modes under sinusoidal wave excitation. The paper poses a theoretical model and presents simulations of different models. The vector method is used to analyze the MA signal amplitude and phase characteristics of the sonic source. Experimental studies of wire sample validate the method.

This study sets a foundation for using low-frequency sinusoidal wave excitation with high accuracy and SNR to study the distribution imaging of tissue's electrical parameters. This method also aids in locating the sonic source of a biological current, and in reconstructing neural activity.

2. Theory

The magneto-acoustic effect is modeled by the wave equation. For the excitation $S(j\omega)$, the wave equation in the frequency domain is [14]

$$\nabla^2 \boldsymbol{P}(\boldsymbol{r}, j\omega) + (\omega^2/c^2)\boldsymbol{P}(\boldsymbol{r},\omega) = (\nabla \cdot \boldsymbol{F})S(j\omega)H(j\omega) \tag{1}$$

Where $p(\boldsymbol{r},t)$ is the MA signal and $\boldsymbol{F}$ is the Lorentz force density in the sample. $\boldsymbol{F} = \boldsymbol{J} \times \boldsymbol{B}_0$. $\boldsymbol{J}$ is the current density, $\boldsymbol{B}_0$ is the static magnetic field, and c is the sample's sonic velocity. $H(j\omega)$ is the system function to the magneto-acoustic measuring system.

The source term can be written as a product of a purely spatial and a purely temporal component [15]

$$\boldsymbol{P}(\boldsymbol{r}, j\omega) = -cS(j\omega)H(j\omega)\iiint\limits_{V} dv(\nabla \cdot \boldsymbol{F})\frac{e^{j\omega|\boldsymbol{r}-\mathbf{r}_0|/c}}{4\pi|\boldsymbol{r}_0 - \boldsymbol{r}|} \tag{2}$$

The vector method is based on the rotating vector method in circuit theory [16]. A sinusoidal signal $s(t) = A_1 \sin(\omega_1 t + \omega_1 t_1)$ can be represented as a vector $A_1 + j\omega_1 t_1$ in a complex plane, as shown in Figure 1(a). The real part is $A_1 \sin(\omega_1 t_1)$; the imaginary part is $A_1 \cos(\omega_1 t_1)$.

When the sonic source moves, the distance varies from L_a to L_b and the vector rotates from v_a to v_b. From Eq. (2) it can be deduced that the amplitude will decrease with $1/L$, and phase Φ_b-Φ_a changes linearly because the transmitting time delay is linear to the distance.

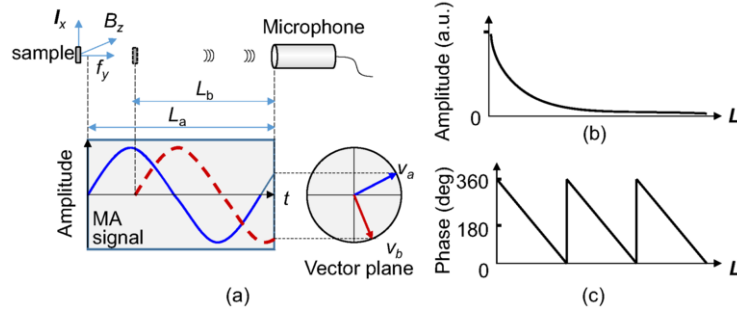$$\Phi_b - \Phi_a = 360°(L_b - L_a)\omega/2\pi c \tag{3}$$

Fig. 1. Theory of magneto-acoustic signal measuring basing on the vector method.

If the medium is considered as a number of separate sonic sources, the summation vector corresponding to the MA signal formed by several sonic sources is the summation of the real and imaginary part for each vector in the complex plane. For the i-th discrete sonic source,

$$\boldsymbol{P}_i(r, j\omega) = (1/L_i)\boldsymbol{f}(r, j\omega)A_i e^{j\omega_1 l_i/c} \tag{4}$$

$$\boldsymbol{f}(r, t) = -(1/4\pi)\pi c \nabla \cdot (\hat{\boldsymbol{J}} \times \boldsymbol{B}_0) \otimes h(t) \tag{5}$$

The vector form is expressed as:

$$\boldsymbol{P}_i(r, j\omega) = \text{Re}_{Pi} + j \, \text{Im}_{Pi} \tag{6}$$

Where the real part and imaginary part are:

$$\begin{cases} \text{Re}_{Pi} = (1/L_i)\boldsymbol{f}(r, j\omega)A_i \cos(j\omega_1 L_i/c) \\ \text{Im}_{Pi} = (1/L_i)\boldsymbol{f}(r, j\omega)A_i \sin(j\omega_1 L_i/c) \end{cases} \tag{7}$$

We can get:

$$\boldsymbol{P}(r, j\omega) = \sum_i \boldsymbol{P}_i(r, j\omega) = \sum_i \text{Re}_{Pi} + j \sum_i \text{Im}_{Pi} \tag{8}$$

Therefore, the measured amplitude and phase of the MA signal in the continuous mode are:

$$AMP_n = \sqrt{\left(\sum_i \text{Re}_{Pi}\right)^2 + \left(\sum_i \text{Im}_{Pi}\right)^2} \tag{9}$$

$$PHA_n = \arctan\left(\sum_i \text{Im}_{Pi} \Big/ \sum_i \text{Re}_{Pi}\right) \tag{10}$$
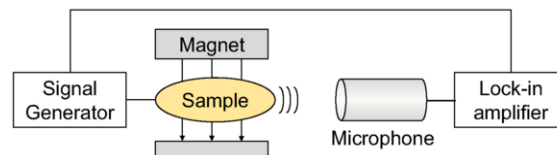
3. Method

Fig. 2. Experimental setup.

3.1. Simulating method

A simulation to line model was used to verify the vector methods and analyze the MA signal characteristics. Based on the discussed above, the amplitude and phase can be calculated using Eqs. (9) and (10). The finite element method (FEM) of a Comsol Multiphysics platform was used in the numerical solution.

3.2. Experimental method

Figure 2 shows the experimental system. A signal generation was used to generate the sinusoid wave (AFG 3252, Tek Co., LTD). The sample was placed in a magnet's magnetic field. The flux density was 0.35 Tesla. A microphone (MP201, BSWA Co., LTD) received the MA signal. A lock-in amplifier (LI5640, NF Co., LTD) measured the amplitude and phase of the MA signal.

To validate the vector method and the simulation results, a copper wire sample was used in the preliminary experiments.

4. Results

4.1. Simulating results

4.1.1. Single sonic source simulation

To simulate the tissue surface or the electrical current, a linear sonic source was used as the simulating model. For a directional microphone, the linear source was simplified as a single source segment in the simulation.

For a single sonic source, the amplitude and phase of the MA signal from the sonic source with different positions, according to Eqs. (2) and (3), it is easily to deduce that, the amplitude decay with distance with $1/L$ trend, while the phase varies linear with distance. The phase variation trend was different at different frequencies. For a simple single sonic source, simulation results and experimental results were compared in section 4.2.

4.1.2. Two sonic sources simulation

Two parallel current clusters were excited to simulate two tissue layers. When the two-layered boundary acoustic sources are a and b, the amplitudes of are both 1 kgS^{-2}m^{-3}. A microphone was placed perpendicularly 1mm away from sonic source b, and the distance between the microphone and the sonic source a gradually increased from 1 mm to 100 mm at 1mm steps. Figure 3 shows the simulation of the MA signal amplitude and phase at different distances.

The simulation results showed that vector v_b corresponding to the MA signal from the sonic source b exhibited a $1/L$ decreasing amplitude trend as distance increasing; the phase decreased linearly with distance. Vector v_a of sonic source a was constant due to the amplitude and because the measuring
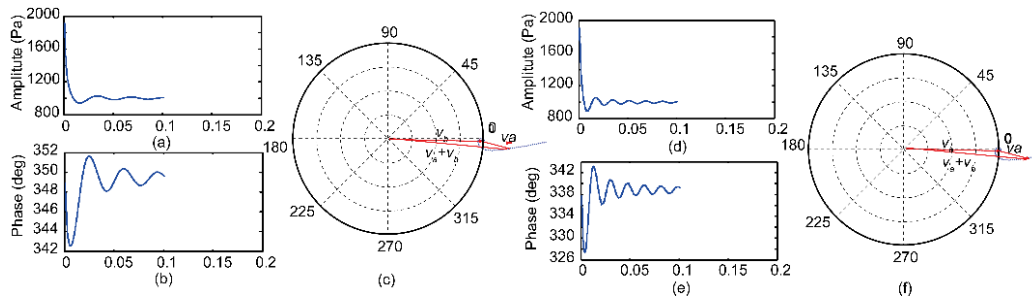
Fig. 3. Simulation results of two sonic sources.

Note: (a) is the simulated amplitude of the MA signal with different detecting distances under 10 kHz excitation.
(b) is the simulated phase of the MA signal with different detecting distances under 10 kHz excitation.
(c) is the vector analysis of (a) and (b) using the vector method.
(d) is the simulated amplitude of the MA signal with different detecting distances under20 kHz excitation.
(e) is the simulated phase of the MA signal with different detecting distances under 20 kHz excitation.
(f) is the vector analysis of (d) and (e) using the vector method.

distance was unchanged.

The amplitude and phase showed periodic increases and decreases due to the rotating vector of v_b. The period was the same as the wave length excitation. The maximum and minimum amplitude values occurred at the phase differences of $180°+n×360°$ and $n×360°$ (n=0, 1, 2 …). The ultimate values of the amplitude and phase equaled the v_b because the v_a amplitude was nearly zero due to a is at infinity far.

Also, it can be seen that the trend was different at 10 kHz and 20 kHz excitation frequencies. The possible cause for this was that the high frequency made the v_a changing period shorter than the low frequency.

4.2. Experimental results

4.2.1. Single wired sample

A 10 mm-long wire was used as an experimental sample. The current was set to 20 mA. The stimulating frequencies were 10 kHz and 20 kHz. The flux density of the static magnetic field was 0.35 Tesla. The commercial microphones contained nickel, which was susceptible to the magnetization detection. The measuring distance from the sound source was set to 60 mm-125 mm in the experiments to avoid the magnetization effect.

As Figure 4 shows, different source locations have different phases formed by the propagating time delay. The phase curve period corresponded with the MA signal frequency. The experimental results are in accordance with the simulation. The phase change related to the frequency, which is in
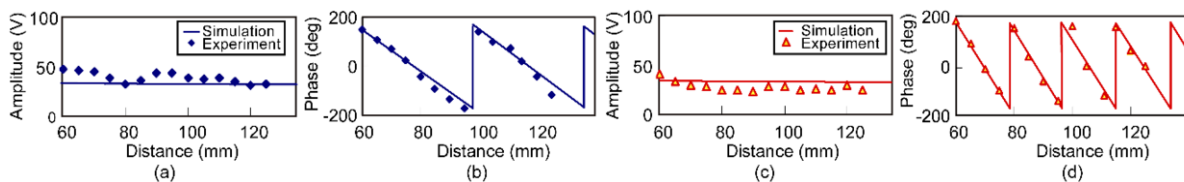

Fig. 4. Experimental result of the wire sample.

Note: (a) is the measured amplitude with different measuring distances. The excitation frequency was 10 kHz.
(b) is the measured phase with different measuring distances. The excitation frequency was 10 kHz.
(c) is the measured amplitude with different measuring distances. The excitation frequency was 20 kHz.
(d) is the measured phase with different measuring distances. The excitation frequency was 20 kHz.

accordance with Eq. (3). The phase changes were 10.6° and 21.2° at 10 kHz and 20 kHz, respectively, when the distance change was 1mm. The error between the theory and measured phases were 5.7% and 2.5% at two frequencies. The repeating periods were 37 mm and 17.2 mm of 10 kHz and 20 kHz, respectively, which related to the frequency.

On the other hand, with increasing distance, the amplitude showed a $1/L$ decay trend at both frequencies. The noise interference and attenuation created deviations between the experiments and the simulated value. This error can be reduced by shielding noise.

The results indicated that the sonic source location can be obtained by measuring the amplitude and phase of the MA signal.

4.2.2. Multi-wired sample

The MA signal of a set of three parallel wires was measured to study and validate the summing characteristic of the sonic sources.

A 10 mA current was applied to three copper wire samples. The exciting frequencies were 10 kHz and 20 kHz. The intervals of No. 1, No. 2, and No. 3 sonic source were 5 mm. Each wire was 10mm long. The microphone pointed perpendicularly to the wire. The measuring distance of the three sonic sources were 100 m, 105 mm, and 110 mm.

Because the shape differences between the wired samples resulted in amplitude and phase errors, a calibration was taken to eliminate the difference by measuring the three wires at the same position.

Figure 5 shows the experimental results and theoretical calculations.

The experiment validated the rules of vector triangle, and the simulation results. The error was within ± 10% due to system noise and measurement errors.

Meanwhile, considering summed sources formed by 1+2 and 2+3, it can be seen that the summed amplitudes of A_{1+2} and A_{2+3}, also the phases Φ_{1+2} and Φ_{2+3}, can be seemed as an integral source moving 5 mm. It means the amplitude and phase can be seemed as an integral source due to the same interval of the single source.

Also, the measured amplitude and phase at 10 kHz and 20 kHz were different, which implied that the sonic source could be reconstructed using multi-frequency measurements.
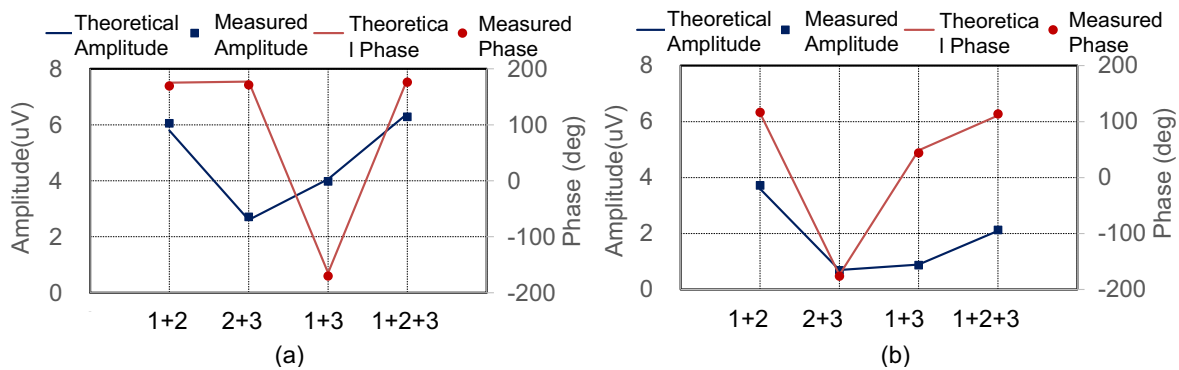

Fig. 5. Experimental results of the mi-sonic source.

Note: (a) is the measured amplitude and phase at 10 kHz.
(b) is the measured amplitude and phase at 20 kHz.
The measured amplitudes were 3.60, 2.61, and 0.71 of sources a, b, and c at 10 kHz;
The measured phases were 179.98º, 155.17º, and -115.02º of sources a, b, and c at 10 kHz;
The measured amplitudes were 2.01, 2.20, and 1.60 of sources a, b, and c at 20 kHz;
The measured phases were 95.10º, 138º, and -60.02º of sources a, b, and c at 20 kHz.

5. Conclusion and discussion

This paper presents a new vector method to determine MA signals. The paper also established a theoretical model and presents simulations. Experiments were conducted with copper wire samples to verify the theory and simulation.

The results showed that when using low-frequency continuous sinusoidal wave modes, the amplitude and phase of the MA signal contained sonic source distribution information. By measuring the amplitude and phase, the intensity and position of the sonic source can be measured and located. The results also verified the vector method and theory.

Follow-up work should be done in further studies. Firstly, real biological tissue experiments must be conducted to study the characteristics of the MA signal from the complex sonic source. Secondly, noise shielding should be improved to reduce measurement errors. Thirdly, based on the characteristics of the MA signal, research should be conducted on using the magneto-acoustic method to reconstruct the sonic source using amplitude and phase.

This study sets a foundation for studying the distribution imaging of tissue electrical parameters using low-frequency sine wave excitation with high accuracy and SNR. It also helps in locating the sonic source of a biological current through the magneto-acoustic method.

References

[1] H. Wen, J. Shah and R.S. Balaban, Hall effect imaging, IEEE Transactions on Biomedical Engineering **45** (1998), 119-124.
[2] B. Roth and P. Basser, A theoretical model for magneto-acoustic imaging of bioelectric currents, IEEE Transactions on Biomedical Engineering **41** (1994), 723-728.
[3] J.F. Emerson, D.B. Chang, S. McNaughton, J.S. Jeong, K.K. Shung and S.A. Cerwin, Electromagnetic acoustic imaging, IEEE Transactions on Ultrasonics, Ferroelectrics and Frequency Control **60** (2013), 364-372.
[4] X. Sun, F. Zhang, Q. Ma, J. Tu and D. Zhang, Acoustic dipole radiation based, conductivity image reconstruction for magnetoacoustic tomography with magnetic induction, Applied Physics Letters **100** (2012), 024105.
[5] N. Narayana, Elements of Engineering Electromagnetics, China Machine Press, Beijing, China, 2006, pp. 35-37.
[6] M.S. Aliroteh, G. Scottt and A. Arbabian, Frequency-modulated magneto-acoustic detection and imaging, Electronics letters **50** (2014), 790-792.
[7] B. Roth, The role of magnetic forces in biology and medicine, Experimental Biology and Medicine **236** (2011), 132-137.
[8] G. Hu, E. Cressman and B. He, Magnetoacoustic imaging of human liver tumor with magnetic induction, Applied Physics Letters **98** (2011), 023703.
[9] L. Mariappan, G. Hu and B. He, Magnetoacoustic tomography with magnetic induction for high-resolution bioimepedance imaging through vector source reconstruction under the static field of MRI magnet, Medical Physics **41** (2014), 022902.
[10] S. Wang, S. Zhang, R. Ma, T. Yin and Z. Liu, A study of acoustic source generation mechanism of magnetoacoustic tomography, Computerized Medical Imaging and Graphics **38** (2014), 42-48.
[11] H. Ammari, Y. Capdeboscq, H. Kang and A. Kozhemyak, Mathematical models and reconstruction methods in magneto-acoustic imaging, European Journal of Applied Mathematics **20** (2009), 303–17.
[12] M. Salim, E. Supriyanto, J. Haueisen, I. Ariffin, A.H. Ahmad and B. Rosidi, Measurement of bioelectric and acoustic

profile of breast tissue using hybrid magnetoacoustic method for cancer detection, Medical & Biological Engineering & Computing **51** (2013), 459-466.

[13] B. Towe and M.R. Islam, A magneto-acoustic method for the noninvasive measurement of bioelectric currents, IEEE Transactions on Biomedical Engineering **35** (1988), 892-894.

[14] G. Hu and B. He, Magnetoacoustic imaging of electrical conductivity of biological tissues at a spatial resolution better than 2 mm, Plos One **6** (2011), e23421.

[15] Y. Xu and B. He, Magnetoacoustic tomography with magnetic induction (MAT-MI), Institute of Physics Publishing **50** (2005), 5175-5187.

[16] E.C. Craig, Electronics via Waveform Analysis, Springer Verlag, US, 1993, pp. 315-317.